Volume 12, Issue 4, Page 1-10, 2023 https://doi.org/10.46810/tdfd.1329067 Research Article

BİNGÖL UNIVERSITY

Türk Doğa ve Fen Dergisi
Turkish Journal of Nature and Science
www.dergipark.gov.tr/tdfd

Hubless Wheel Design and Calculations

Said Bera ÇİVİ[1*], Veysel TÜRKEL[2]

[1]Osena Mobilya Aksesuarları Ltd. Şti, Esenyurt, İstanbul
[2]İstanbul Teknik Üniversitesi, ARDES, Maslak, Sarıyer, İstanbul
Sait Bera ÇİVİ ORCID No: 0000-0002-1040-8689
Veysel TÜRKEL ORCID No: 0000-0003-4174-1406

Corresponding author: turkelv@itu.edu.tr

(Received: 18.07.2023, Accepted: 8.10.2023, Online Publication: 28.12.2023)

Keywords
Helicar gear,
Stabilization,
Mechanical design

Abstract: In this study, Helical gear design, analysis and calculations, chain gear system design and calculations, lubrication system, brake disc, caliper, original stabilization part and system, transmission shaft design, calculations and analysis, wedge calculations analysis and design, bearing, ring selection and necessary information about dimensioning of the system, mechanical design, system components and methods are presented. The advantages and disadvantages of the system compared to conventional wheels have been reviewed and a cost analysis has been made. Since the system has a disadvantageous efficiency compared to traditional wheels, it has been tried to increase the efficiency and life of the current design and to create a usage area in the market.

Göbeksiz Tekerlek Tasarımı ve Hesaplamaları

Anahtar Kelimeler
Helisel dişli,
Stabilizasyon,
Mekanik dizayn

Öz: Bu çalışmada, Helisel dişli, zincir dişli sistemi, yağlama sistemi, fren diski, kaliper, özgün stabilizasyon parçası ve sistemi, aktarma mili tasarımı, kama hesapları, analizleri ve tasarımları yanı sıra rulman, segman seçimi ve sistemin boyutlandırılması, mekanik dizaynı, sistem bileşenleri ve yöntemleri hakkında gerekli bilgiler verilmiştir. Sistemin geleneksel tekerleklere kıyasla avantaj ve dezavantajları gözden geçirilmiş ve maliyet analizi yapılmıştır. Bu analiz sonucunda sistem geleneksel tekerleklere göre dezavantajlı verime sahip olması sebebiyle güncel tasarımın verimi ve ömrü arttırılmaya çalışılarak piyasa içerisinde bir kullanım alanı oluşturmak amaçlanmıştır.

1. INTRODUCTION

A hubless wheel refers to wheel designs that do not have a rotating hub at the center of the wheel. The advantages of using such a wheel include reducing the rotating inertia of the wheel and creating an empty space by eliminating the spoke wires and weights inside the hub used in motorcycle rims [1]. Additionally, this design is much more appealing compared to traditional wheel designs. This design was initially invented by Franco Sbarro [2,3], the founder of Sbarro automobiles, in 1989, and during that time, it gained recognition for its striking appearance. However, hubless wheels, compared to traditional wheels, come with disadvantages such as the complexity of manufacturing, more components involved, increased calculation requirements, and higher costs. These factors pose obstacles to their alternative and widespread use and development. The existing drivetrain system found in current cars is problematic because the options for transferring power in traditional systems are limited to belt pulleys or chain gears, which do not allow the use of axles and constant velocity joints [4-6]. In addition, in the 2010 film Tron: Legacy, scenes featuring hubless wheeled motorcycles were showcased with the inclusion of light animations, which brought the concept of hubless wheels back into the spotlight within the automotive industry. The company responsible for the motorcycle design in the film, Hammacher Schlemmer, stated that many people were fascinated by the wheels of the motorcycle and that numerous manufacturing companies sought inspiration from them [7,8]. This film inspired many engineers and companies to start developing new designs. To add a new design element to this unique concept and to treat it as a thesis project, a decision was made to design a hubless wheel.

The aim of this study is to achieve a durable, long-lasting, and original design from mechanical and intricate hubless wheels and, most importantly, to create a new market niche. Among these goals are the entertainment industry, racing tracks, and everyday usage. If successful results are obtained from this project, it will not only lead to high-value production but also create employment opportunities in various regions of our country. Additionally, when increased energy production and the electric vehicle sector come together, it will significantly reduce our unemployment rate. This will demonstrate to the world that we exhibit an innovative approach rather than traditionalism, contributing to our country in many aspects. These contributions include inspiring various industries, including the existing automotive sector. Furthermore, this design highlights the necessity of promoting high-value product manufacturing within Turkey.

2. MATERIAL AND METHOD

There are four important factors to consider in the design of the system, these are:
- Transmission System
- Lubrication System
- Stabilization
- Brake System

2.1. Transmission System

One of the key aspects of the system is how the initial power from the engine will be transferred. Hubless wheel designs require the necessity of working with rotating motion and torque transfer, such as belts, pulleys, or chain gears. Instead of focusing on solving this problem, it was deemed more suitable to adapt the design from cars to motorcycles. The second aspect is how the power obtained from the chain gear will be transmitted to the wheel. Many designers have chosen to transfer the power from the engine to the traditional wheel located at the rear, rather than the hubless wheel. As an alternative to this choice, it is considered beneficial to design a large gear that matches the diameter of the rim and mount the gear directly onto the rim when transferring power with a chain gear.

If it is possible to provide the transmission through a large hubless chain gear, this design approach will significantly reduce the number of parts and costs. With this design, components such as the drive shaft, pinion, internal helical gear, auxiliary bearing, segments, and wedges will no longer be needed. However, the transition from a small gear to a large gear will still result in a significant RPM drop. To overcome this issue, a reducer of the same size or motor power should be planned and designed. However, the standard power of motors available in the market is limited to a maximum of 3000 RPM. Therefore, within the existing transmission system, two helical pinion gears placed on the drive shaft and two internal helical gears connected to the rim are used for power transmission.

2.2. Lubrication Issue

Another problem of hubless wheels is the lubrication issue. The biggest criticism of this system is that, unlike traditional wheels, no matter how much manual lubrication is applied, the system still experiences dry friction. Additionally, due to the presence of more interacting components compared to traditional wheels, friction is significantly increased. Moreover, due to the open nature of the hubless system, the transmission components are more exposed to foreign particles from the outside. The solution method identified for this problem is to ensure sealing only at the points where the transmission occurs. This is referred to as transitioning to a lubrication method while the entire system is closed. Lubrication calculations were performed to address this issue, and a closed lubrication system was deemed necessary for long-term durability.

2.3. Stabilization

Once the general design of the hubless wheel is completed, the following questions arise: How will the wheel be connected to the engine? Will it be able to maintain a stable and smooth movement while also accommodating the chain gear design? What should the design be like? Where should the bearing of the drive shaft be located? Will there be any friction during these processes? These questions need to be addressed. Stabilization is the most crucial component of the system, responsible for keeping the system together and creating a socket for attaching the wheel system to the chassis. In the assembled system, there are bearings in the form of balls that serve as the connection between the rim and the stabilization component. These balls, similar to the gears, are subjected to a closed lubrication system and are designed to be suitable for production and assembly. The axle connection and bearing housing points, which will connect the chassis to the wheel, are also present on the stabilization component.

2.4. Brake System

In previous designs, the braking system was not integrated into the system. This was due to the lack of designed brake discs and calipers that would be suitable for the system. Additionally, the brake system was not separated from the lubrication system. Therefore, it was decided that the use of a closed lubrication system would prevent oil from coming into contact with the brake disc. The brake system in the design is located in the center of the hub. This is made possible by the closed design of the lubrication system and the unique components used in the brake system. When looking at other Hubless Wheel designs, it can be observed that the brake caliper and disc are located either on the right or left, similar to traditional wheels. However, in this new design, moving the brake caliper and disc to the center of the system is crucial to balance the stresses that occur during braking.

3. RESULTS

Taking a general overview of the design, it consists of several key elements: the initial power provided by the electric motor connected to the chassis, the transmission of the driving force to the drive shaft through the chain gear, the rotation of the drive shaft with the help of wedge, bearing, and segment auxiliary materials, and the engagement of two helical pinion gears fixed to the drive shaft. The pinion helical gears start rotating the internally fixed helical gears on the rim at a gear ratio of i=4.17. Simultaneously, the brake disc connected to the internal helical gear starts rotating with the system. However, the caliper is fixed to the lubrication chamber to ensure its stability.

Based on the calculations, the required motor power is determined to be 8 kW. The motor output torque is 1456 Nm, and its speed is 1200 rpm. Under these conditions, the analysis has been conducted to calculate the environmental forces and the values of the external forces (Figure 1 and Figure 2).

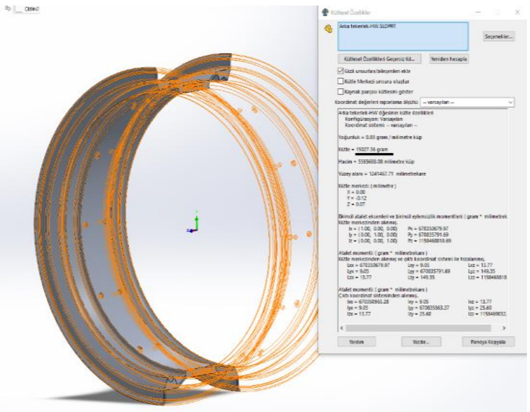

Figure 1. Mass measurement results of hubless rim design

Hubless rim design;

$$m = 14{,}07\,kg$$
$$r_1 = 260mm$$
$$r_2 = 274{,}25\,mm$$
$$I_z = \frac{1}{2} \times m \times (r_1^2 + r_2^2) = \frac{1}{2} \times 14{,}07 \times (260^2 + 274{,}25^2)$$
$$= \mathbf{998732\;kgmm^2}$$
$$\boldsymbol{I_X = \frac{1}{12} \times m \times \left(3(r_1^2 \times r_2^2) + h^2\right) = 1/12 \times 14 \times (3 \times (260^2 + 274,5^2) + 257,82^2)}$$
$$\boldsymbol{= 576423,1687\;kgmm^2} \qquad (1)$$

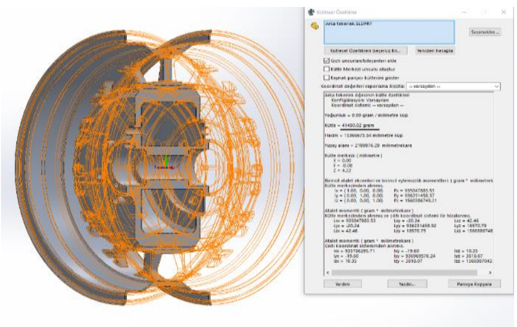

Figure 2. Estimated rim mass measurement with hub motor mounted.

Hub Motor Rim design;

$$m = 47{,}89\,kg$$
$$r = 280mm$$
$$\boldsymbol{I_z = m \times \frac{r^2}{2} = 47,89 \times \frac{280^2}{2}} \qquad (2)$$
$$\boldsymbol{= 1842400\;kgmm^2}$$
$$I_x = \frac{m}{12} \times (3 \times r^2 + h^2) = \frac{47{,}89}{12} \times (3 \times 280^2 + 257^2)$$
$$\boldsymbol{= 1179891,917\;kgmm^2}$$

According to the results obtained, the hubless wheel, compared to the hubless motorized wheel, has an advantage in terms of the moment of inertia.

3.1. Design Elements

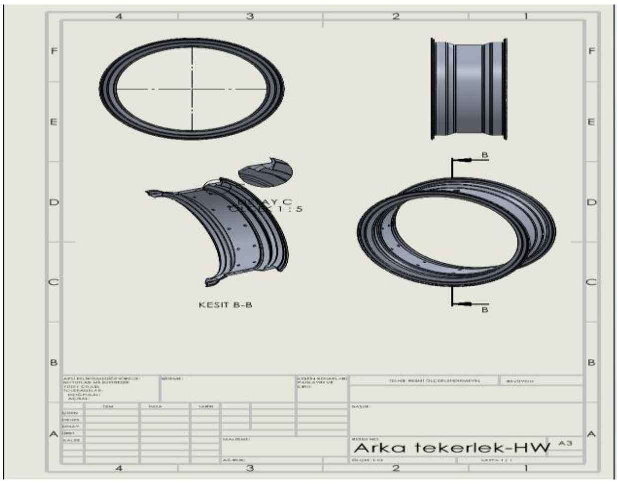

Figure 3. Rim Technical Drawing

Aluminum alloy, specifically Aluminum 1060 Alloy, has been chosen as the material for the wheel rim due to its widespread use in the automotive industry. This alloy consists of approximately 90% aluminum and 10% silicon. It may also contain trace amounts (less than 1%) of titanium, magnesium, and other metals. Aluminum 1060 Alloy is deemed suitable for use as a rim material due to its strength values and lightweight characteristics, as shown in Table 1.

Table 1. Rim Material Values

Material	Aluminum 1060 Alloy
Tensile Strength	68,9356 Mpa
Yield Strength	27,5742 Mpa
Crushing Strength	Pem = 13,7871 Mpa

The rim has metric 6 bolt holes on its inner side. The assembly of internal helical gears is done in these holes. When looking at the auxiliary view of section B-B, a separate circular void is observed, which is placed between the part that provides stabilization of the wheel and the rim. To prevent friction and ensure movement capability, sockets have been created for the bearings.

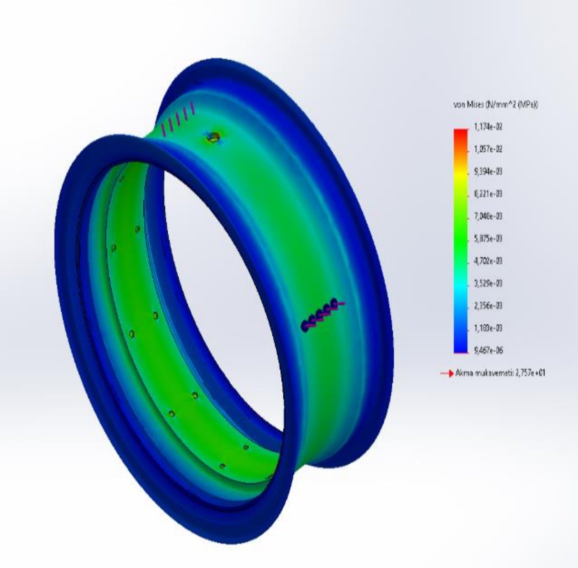

Figure 4. Rim Strength Analysis-1

Table 2. Rim Analysis Results-1

Safe crushing stress	13,5784 Mpa
Yield strength	27,5742 Mpa
Maximum tension	$1{,}174 \times 10^{-1} Mpa$
Minimum tension	$9{,}467 \times 10^{-6}\ Mpa$

Figure 5. Rim Strength Analysis-2

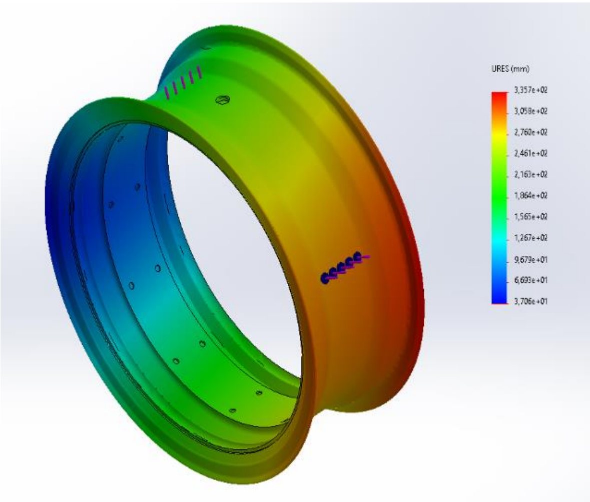

Table 3. Rim Analysis Results-2

Maximum amount of deflection	**Minimum amount of deflection**
33,57mm	3,706 mm

The results of the strength and deflection analyses conducted in Figures 4 and 5 are provided in Table 2 and Table 3, respectively. The results show that the stresses generated are lower than the safe stress limit, indicating that the material and design have sufficient strength.

3.1.1. Stabilization Component

The role of the stabilization component is to house the connection points of the primary transmission elements. It accommodates the connection points of the chain sprocket, which transfers power from the engine to the wheel, and the shaft, which transfers rotational force from the gear to the reducer.

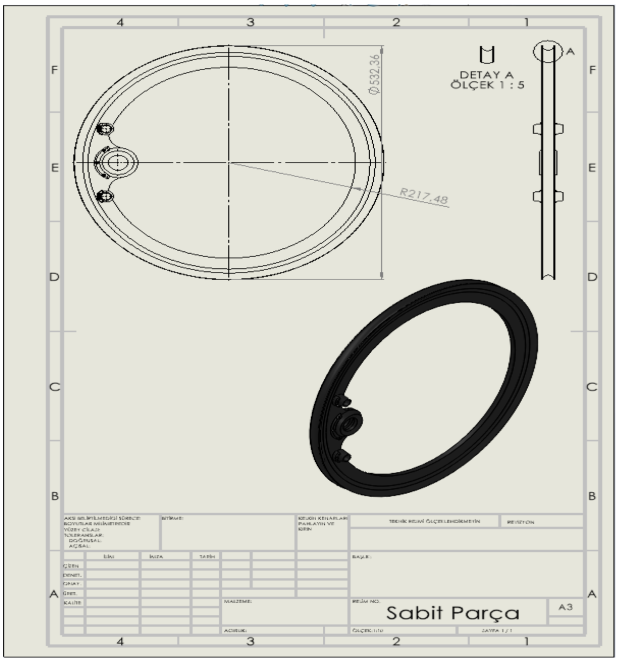

Figure 6. Stabilization Piece Technical Drawing

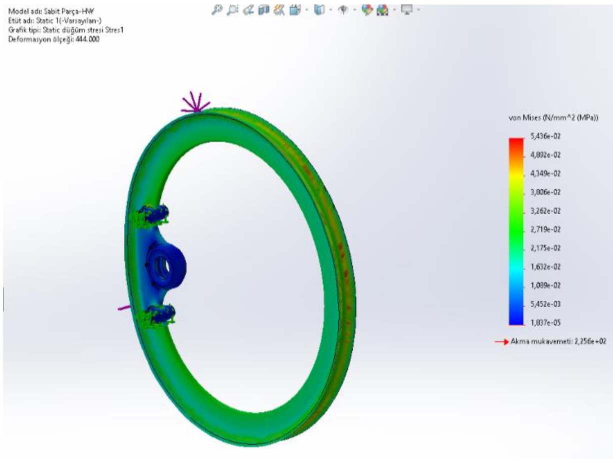

Figure 7. Equivalent stress view

Table 4. Equivalent stress results

Yield strength	Safe crush strength	Maximum stress	Minimum stress
225,6 Mpa	45,12 Mpa	$5{,}346 \times 10^{-2} Mpa$	$1{,}837 \times 10^{-5} Mpa$

As seen in Figure 7 and Table 4, the maximum stress obtained from the equivalent stress analysis falls within the safe strength range, ensuring safety.

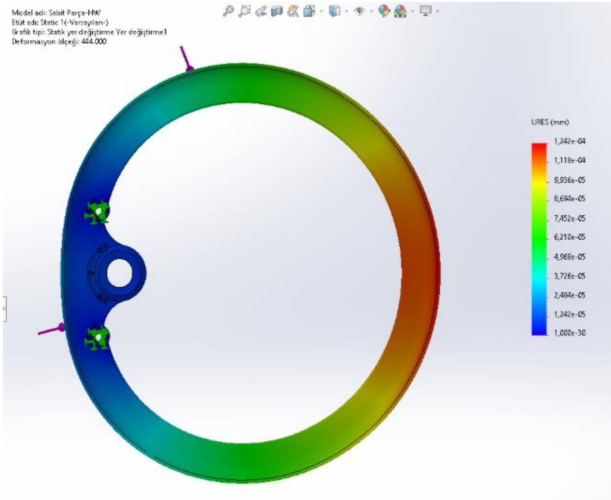

Figure 8. Deflection view

Table 5. Deflection amount

Maximum deflection	Minimum deflection	Deformation scale
$1{,}242 \times 10^{-4} mm$	$1 \times 10^{-30} mm$	444.000

The deflection amount is a deformation scale that needs to be considered. As can be understood from Figure 8 and Table 5, in order to make the resulting deformation visible to the naked eye, it has been added to the representation with a magnification of 444,000 times.

3.2. Necessary Calculations for Helical Gears

The dimensioning of the helical gear mechanism is based on the gear ratio i = n1/n2 = 1750/408 = 4.2892 and the torque M = 42.7358 Nm.

3.2.1. Pressure angle

The pressure angle of standard-sized helical gears is $\alpha_n = 20^o$

3.2.2. Helix angle

If β is small, efficiency increases and the added load decreases. However, as β increases, the engagement path lengthens, leading to multiple teeth engaging simultaneously. When necessary, the gear can be narrowed by increasing β. β is taken as 15°.

3.2.3. Face width coefficient

Table 6. Width Coefficient Based on Surface Finish and Shaft Bearing Condition (Bozacı et al., 1989)

Surface Finish and Bearing Condition	ψ_m	ψ_d
Unprocessed Cast Gears	**4÷5**	**0,23÷0,28**
Processed Gears	**7÷9**	**0,4÷0,5**
Precision Processed Gears	**14÷16**	**0,7÷0,9**
Precision Processed Gears with Bearings on Both Sides	**18÷23**	**1÷1,3**
Precision Processed Helical Gears with Bearings on Both Sides	**20÷40**	**1,1÷2**

Note: ψm is taken as 20 using the last row of Table 6.

3.2.4. Number of teeth on the driving gear

For the purpose of counting in the normal plane, $Z_1 = 28$.

3.2.5. Form factor K_{fn}

Table 7. K_{fn} form factor ruler according to the number of teeth for $\alpha_n = 20°$ for DIN 867 (Bozacı vd., 1989)

Z	**13**	**14**	**15**	**16**	**18**	**20**	**22**	**24**
$\mathbf{K_{fn}}$	3,5	3,3	3,23	3,85	3,4	2,95	2,85	2,78
Z	**26**	**28**	**30**	**35**	**40**	**50**	**70**	**100**
$\mathbf{K_{fn}}$	2,7	2,64	2,6	2,51	2,4	2,37	2,28	2,2

Theoretical equivalent will be selected according to the number of teeth. For $z_n = \frac{z_1}{cos^3\beta} = \frac{28}{cos^3 15} = 31{,}06 \cong 31$ pieceses, K_{fn} is taken 2,65 from Table 7 by interpolation.

3.2.6. Profile grip ratio

For $a_n = 20°$ ve $\beta = 15°$ ε is taken as 1,65

3.2.7. Number of dynamic loads

K_d is taken as 1.16, assuming that the workmanship is sensitive and the peripheral speed is $\frac{1750}{60} = 29{,}16\ cycle/s$ and $29{,}16 \times 2 \times 3{,}14 \times 0.113926 = 20{,}86\frac{m}{s} \cong 21\ m/s$. The overload safety factor (S) is taken as 1.25.

3.2.8. Material

One of the most sought-after characteristics in gear wheels is hardness. Both gears were selected to be made of Ck 60 material. Yield $\sigma_{Ak} = 390\frac{N}{mm^2}$, rupture $\sigma_k = 700\frac{N}{mm^2}$, hardness $H_B = 2410\frac{N}{mm^2}$. $\sigma_D \approx 0{,}5 \times \sigma_K = 350\frac{N}{mm^2}$. $\sigma_{em} = \frac{\sigma_D}{K_ç} = \frac{350}{1{,}5} = 233\frac{N}{mm^2}$ The pressure that can be transported safely is taken as $P_{em} = 0{,}25H_B = 602\frac{N}{mm^2}$.

3.2.9. Moment to be transmitted

Moment $M = 42{,}7358\ Nm$ = 42735,8 Nmm, conversion Rate $i = 4.2892$

3.2.10. Determining the modüle

According to the gear bottom strength;

$$\boldsymbol{m_n} = \sqrt[3]{\frac{\mathbf{2} \times \boldsymbol{S} \times \boldsymbol{M_{d1}} \times \boldsymbol{K_D} \times \boldsymbol{K_{fn}} \times \boldsymbol{cos\beta}}{\boldsymbol{z_1} \times \boldsymbol{\psi_m} \times \boldsymbol{\sigma_{em}} \times \boldsymbol{\varepsilon}}}$$

$$= \sqrt[3]{\frac{\mathbf{2 \times 1{,}25 \times 42735{,}8 \times 1.6 \times 2{,}65 \times cos15°}}{\mathbf{28 \times 20 \times 233 \times 1{,}65}}} = 1.2319\ mm (3)$$

According to abrasion and crushing, m_n has been obtain as following;

$$\boldsymbol{m_n} = \sqrt[3]{\frac{2 \times S \times M_{d1} \times E \times K_d \times cos^4\beta}{z_1^2 \times P_{em} \times \varepsilon \times \psi_m} \times \frac{i+1}{1}} \tag{4}$$

$$m_n = \sqrt[3]{\frac{2 \times 1{,}25 \times 42735{,}8 \times 2{,}1 \times 1{,}6 \times cos^4 15°}{28^2 \times 602^2 \times 1{,}65 \times 20} \times \frac{4{,}2982+1}{1}}$$

$$= 1{,}4937\ m$$
$$m_n = 2\ mm$$

3.2.11. Dimensioning

Table 8. Gear Dimensioning Table

Dimensioning parameters	Driving gear	Driven gear
Normal module	2mm	2mm
Forehead Module	2,07	2,07
Tooth width	41,4110	41,4110
Rolling circle diameter	115,92	453,68
Number of teeth	28 pieces	122 pieces
Head circle diameter	119,92	457,63
Base circle diameter	110,92	448,68

3.2.12. Forces acting on shaft bearings

Perimeter force $\boldsymbol{F_p = 2 \times S \times \frac{M_{d1}}{d_1} = 2 \times 1,25 \times \frac{42{,}7358}{50{,}68} = 2108\ N}$ (5)

(6)

Tooth force $\boldsymbol{F_t = \frac{F_Ç}{\cos(a_n) \times \cos(\beta)} = \frac{2108}{\cos(20°)} \times \cos(15°) = 2322,42N}$

(7)

Radial Force $\boldsymbol{F_r = F_z\ sina_n = 2322,42 \times sin20 = 794,17N}$

(8)

Axial Force $\boldsymbol{F_a = F_ç \times tg\beta = 2108 \times tg15 = 564,83\ N}$

3.3. Calculations Required for Wedge

Wedge refers to the small components that allow the connection of elements such as gears, pulleys to shafts in a detachable manner, enabling the transmission of motion from the shaft to the hub or from the hub to the shaft. Among the types of wedges, the embedded key is the most commonly used and cost-effective type available in the market. Therefore, an embedded key has been used in the design.

3.3.1. Calculation of wedge length

The only calculation required for fit wedges is the determination of the wedge length.

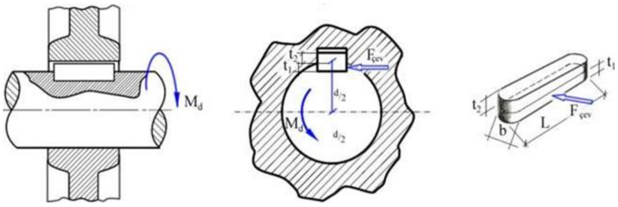

Figure 9. Forces and Dimensioning of Fit Wedges

If the $t_1 \times L$ surface is subjected to crushing, either the shaft or the hub will be crushed. To prevent damage to the shaft, the wedge material should be chosen weaker than the shaft.

$$\boldsymbol{P = \frac{F_{çev}}{A_1} = \frac{F_{çev}}{L \times t_1}} \tag{9}$$

The same calculation should also be performed for the $t_2 \times L$ surface, and in this calculation, the crushing of the wedge or the hub should be checked to prevent damage.

$$\boldsymbol{P = \frac{F_{çev}}{A_2} = \frac{F_{çev}}{t_2 \times L}} \tag{10}$$

Calculations should be performed to assess the lateral crushing of the wedge. The intersection point of the hub and the shaft should also be checked to ensure that the hub shaft is not cut or damaged.

$$\boldsymbol{T = \frac{F_{çev}}{A_3} = \frac{F_{çev}}{b \times L}} \tag{11}$$

The longest among the three wedge lengths should be considered as the reference for the wedge length in these calculations. Additionally, one of the upper limits from the standard wedge lengths should be selected. The standard wedge lengths available in the market are as follows;

L = 6, 8, 10, 12, 14, 18, 20, 22, 25, 28, 32, 36, 40, 45, 50, 63, 70, 80, 90, 100, 110, 125, 140, 160, 180, 200, 220, 250, 280, 315, 355, 400 mm

Figure 10. Standard Dimensions of Fit Wedges

Transfer from sprocket gear to transmission shaft:
RPM = 1750 rpm
Torque = 42.7358 Nm
Safety Factor (S) = Light Impact, Variable Load = 5

$\boldsymbol{Shaft_{material}} = Fe\ 50$
$\sigma_{Ak} = 450 \frac{N}{mm^2}$
$T_{bD} = 150 \frac{N}{mm^2}$
$T_{em} = \frac{150}{5} = 30\ N/mm^2$,
$P_{em} = \frac{\sigma_{ak}}{S} = \frac{450}{5} = 90\ N/mm^2$

$\boldsymbol{Wedge_{material}} = Fe\ 42$
$\sigma_{ak} = 380 \frac{N}{mm^2}$
$T_{bD} = 130 \frac{N}{mm^2}$
$T_{em} = \frac{130}{S} = \frac{130}{5} = 26\ N/mm^2$
$P_{em} = \frac{\sigma_{ak}}{5} = 76 \frac{N}{mm^2}$

$\boldsymbol{Hub_{material}}$ = Fe 50

$\sigma_{Ak} = 450 \frac{N}{mm^2}$

$T_{bD} = 150 \frac{N}{mm^2}$

$T_{em} = \frac{150}{5} = 30\ N/mm^2$,

$P_{em} = \frac{\sigma_{ak}}{S} = \frac{450}{5} = 90\ N/mm^2$

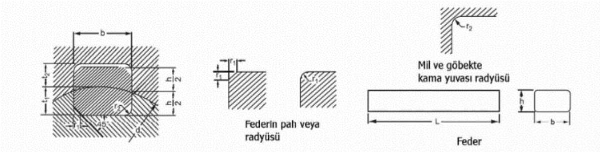

Mil çapları	den büyük	6	8	10	12	17	22	30	38	44	50	58	65	75	85	95	110	130	150	170	200	230	260	290	330	380	440
	e kadar	8	10	12	17	22	30	38	44	50	58	65	75	85	110	110	130	150	170	200	230	260	290	330	380	440	500
Feder kesiti	Genişlik b	2	3	4	5	6	8	10	12	14	16	18	20	22	25	28	32	36	40	45	50	56	63	70	80	90	100
	Yükseklik h	2	3	4	5	6	7	8	8	9	10	11	12	14	14	16	18	20	22	25	28	32	32	36	40	45	50
Yuva derinliği (Nominal)	Milde t_1	1.2	1.8	2.5	3.0	3.5	4.0	5	5	5.5	6	7	7.5	8.5	9.0	10	11	12	13	15	17	19	20	22	25	28	31
	Göbekte t_2	1	1.4	1.8	2.3	2.8	3.3	3.3	3.8	3.8	4.3	4.4	4.9	5.4	5.9	6.4	7.4	8.4	9.4	10.4	11.4	12.4	13.4	14.4	15.4	17.4	19.5
Yuva derinlik toleransı	t_1		+0.05 −0.00					+0.1 −0.0												+0.15 −0.00							
	t_2		+0.05 −0.00					+0.1 −0.0												+0.15 −0.00							
Federin pah veya radyüsü	r max		0.25			0.35			0.55					0.80						1.30			2.00			2.95	
	r min		0.16			0.25			0.40					0.60						1.00			1.60			2.50	
Yuva radyüsü	r_2 max		0.16			0.25			0.40					0.60						1.00			1.60			2.50	
Feder uzunluğu	L min	6	6	8	10	14	18	22	28	36	45	50	56	63	71	80	90	100	110	125	140	160	180	200	220	250	280
	L max	20	36	45	50	71	90	110	140	160	180	200	220	250	280	320	360	400	400	400	400	400	400	400	400	400	400

Figure 11. Wedge Sizes according to Shaft Diameter

Wedge sizes according to shaft diameter:

$$\boldsymbol{d = \sqrt[3]{\frac{16 \times M_d}{\pi \times T_{em}}} = \sqrt[3]{\frac{16 \times 42,78 \times 1000}{3,14 \times 30}} = 19,36\ mm} \tag{12}$$

$Shaft\ Diameter\ (d)$: 20 mm
$Width\ (b)$: 6 mm
$Height\ (h)$: 6 mm
$Shaft\ Depth\ (t1)$: 3.5 mm
$Hub\ Depth\ (t2)$: 2.8 mm

$M_d = F_Ç \times \frac{d}{2}$

$F_Ç = 2 \times \frac{M_d}{d} = 2 \times 42,7358 \times \frac{1000}{20} = 4278\ N$

The wedge length based on the crushing;

$P = \frac{F_Ç}{t_1 \times L}$

$$\boldsymbol{L_{wedge} = \frac{F_ç}{t_1 \times P} = \frac{4278}{3,5 \times 76} = 9,09\ mm} \tag{13}$$

The wedge length based on the shear stress;

$T = \frac{F_{çev}}{A_3} = \frac{F_{çev}}{b \times L}$

$$\boldsymbol{L_{wedge} = \frac{F_{çev}}{T \times b} = \frac{4278}{26 \times 10} = 16,45\ mm} \tag{14}$$

Based on the provided standard wedge length;
L = 18 mm

3.4. Calculations Required for Sprocket Gear

The sprocket gear is the component used to transfer the motor output power to the transmission shaft. It plays a crucial role in the power transmission system. (See Figure 12).

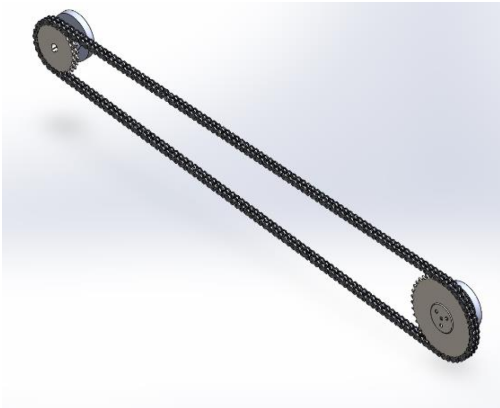

Figure 12. Assembly of Sprocket Gear Transmission

3.4.1. Calculation of chain-sprocket gear (Based on ANSI standards)

1KW = 1,341 Hp
8KW = 10.789 Hp

3.4.2. Operating factor

The machine is considered to have heavy impact loads. Due to being driven by an electric motor $\delta_1 = 1.5$, since it operates in a clean environment $\delta_{2=}1{,}2$, with an estimated operating time of over 10 hours δ_3 = 1,4.

$$\boldsymbol{\delta = \delta_1 \times \delta_2 \times \delta_3} \tag{15}$$

So, it is accepted as follows;
$\delta = 1{,}5 \times 1{,}2 \times 1{,}4 = 2{,}52$

3.4.3. Design power (Hp)

Design power refers to the power that needs to be transmitted with a safety margin

$$\boldsymbol{P_{hes} = P_g \times \frac{\delta}{Sıra\ Katsayısı}} \tag{16}$$

$P_{hes} = 10{,}789 \times \frac{2{,}52}{1} = 27\ Hp$

Pre-selection

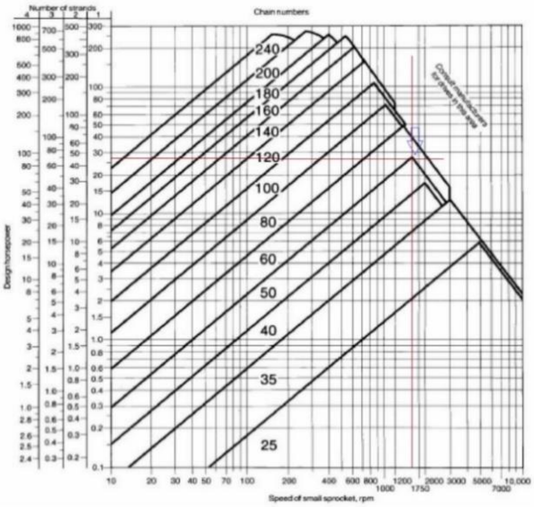

Figure 13. Chain Model Power Diagram

The power diagram, a chain with number 50 was selected for n_1 =1600 rpm $P_{hes} = 27{,}1882\ BG$. The chain pitch (P) was read as (P) = $\frac{5}{8}''$.

3.4.4. Final selection

Based on the power evaluation table, for the given chain with n_1 = 1600 rpm and P_{hes} = 27.1882 hp, it is observed that it guarantees the required power when used with a gear with $z_1 = 20{,}1\ \cong 20$ teeth.

3.4.5. Selection of the driven gear

The gear ratio is calculated as i = 1600/1750 = 0.9142.
The number of teeth on the driven gear is calculated as z_2= i × z_1 = 0.9142 × 20.1 ≈ 18.
Therefore, the driven gear is selected to have approximately 18 teeth.

3.4.6. Chain length

The chain length can be calculated using Equation (17):

$$\boldsymbol{Z = \frac{2a}{P} + \frac{z_2 + z_1}{2} + (\frac{z_2 - z_1}{2\pi})^2 \times \frac{P}{a}} \qquad (17)$$

$$Z = 2 \times \frac{657{,}8}{1} + \frac{18+20}{2} + (\frac{18-20}{2\times3{,}14})^2 \times \frac{1}{657{,}8} = 1333{,}6001 \cong 1334$$

When rounded to the nearest even number, a total of 1334 links will be required for the chain.

3.4.7. Chain maintenance and lubrication

As indicated in the power evaluation table, the chain should be lubricated using the immersion method with a type B oil bath. This method involves immersing the chain in an oil bath for lubrication and maintenance purposes.

3.5. Transmission Shaft Assembly

Table 9. Assigned Material Values for Transmission Shaft

Material	Density	Yield Strength	Thermal Conductivity	Poisson's Ratio
Case-hardened Steel	7800 kg/m^3	8*10^8 N/m^2	14 W/ m*K	0,28

The transmission shaft is supported by bearings at both ends. Due to its location in the hub, analysis is deemed necessary. The resistances considered in the analysis include the resistance caused by initial motion due to friction and acceleration. The stresses and deflections on the shaft caused by the circumferential force of 80 + 80 = 160 N applied to the wedges have been measured.

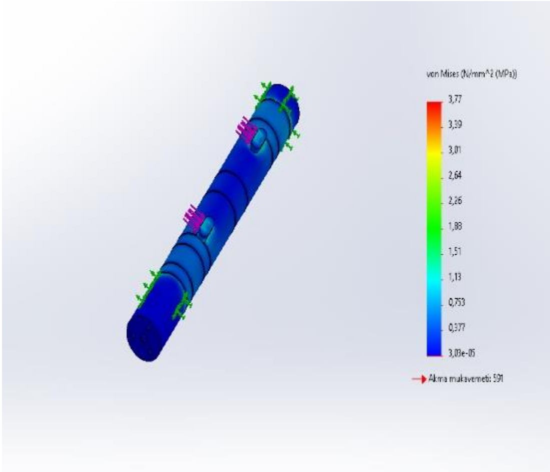

Figure 14. Representation of Equivalent Stress

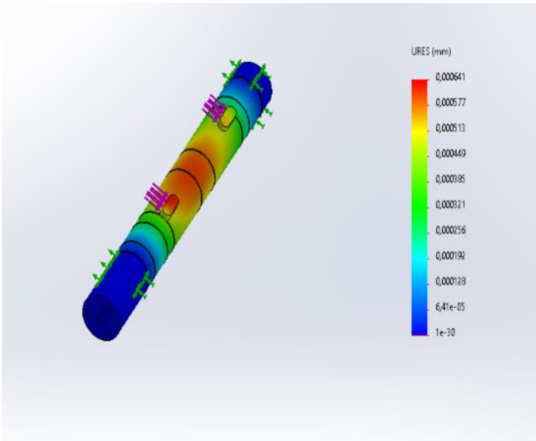

Figure 15. Representation of Displacement of Transmission Shaft

Table 10. Stress Analysis Results

Circumferential Force	Maximum Equivalent Stress	Minimum Equivalent Stress	Maximum Displacement
80 N	3,77 Mpa	0,377 Mpa	0,000641mm

Based on the values provided in Figure 14, Figure 15, and Table 8, the analysis was conducted assuming that the transmission shaft is supported by bearings at both ends and considering two circumferential forces of 80 N applied to the wedges.

3.6. Brake Disc

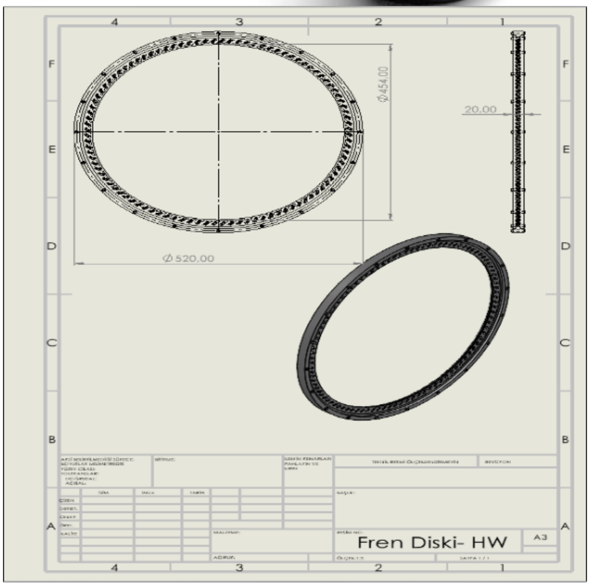

Figure 16. Technical Drawing of Brake Disc

Figure 16 depicts the Brake Disc specifically designed for the system, aiming to be secured by a circumferential loop of 20 M10 bolts.

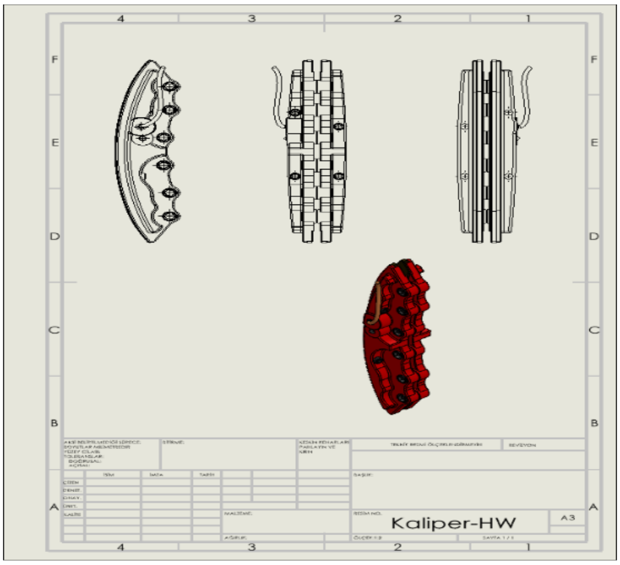

Figure 17. Technical Drawing of Caliper

3.7. Caliper

Figure 17 illustrates a reverse caliper design that differs from standard brake calipers by compressing from inside the frame, rather than from the outside, in accordance with the design of the brake disc. The renders shown in figure 18 were created using Autodesk VRED Pro software.

Figure 18. Hubless Wheel Render views

4. DISCUSSION AND CONCLUSION

The mechanical friction, which was one of the issues in previous versions of the hubless wheel system, has been minimized with the new design. The number of components has been reduced, making the system more manufacturable. The existing advantages and disadvantages of the system have been reevaluated and presented to you in this section with an objective approach. The design includes 2 sets of stabilizers, internal helical gears, and a helical pinion gear, which differentiate it from traditional wheels. Additionally, there are 1 transmission shaft, 4 bearings, 8 segments, 80 ball bearings, 4 sealing components, 2 wedges, and 1 closed lubrication system, totaling 106 additional parts and 10 different components. The excessive number of components compared to traditional wheels leads to mechanical losses, additional cost expenses, and challenges in assembly and production. The additional cost expenses pose a significant problem for both consumers and manufacturers. Everything, from the machinery used in production to the storage space allocated for extra parts, reflects in the prices. Furthermore, the reduced number of components in traditional wheel designs allows for faster and more efficient production processes compared to hubless wheels. From a consumer perspective, the disadvantages include not only the product price but also the need for spare parts that may arise in case of accidents. However, when comparing the hubless wheel to a wheel with a hub-mounted motor, the hubless wheel has an advantage in terms of moment of inertia. Additionally, the design and layout of hubless wheels make it easier for them to find a place in the market. As mentioned in the introduction, many companies, especially in the motorcycle industry, have started transitioning to this design. Efforts are also being made to explore alternative solutions to overcome the disadvantages of this design. It is evident that sacrificing the number of components in the hubless wheel design to reduce costs, ease assembly and production, and increase efficiency makes the Hubless DC electric motor design the most suitable option. The use and application areas of hubless motors are increasing in today's market. This growth encompasses various areas such as bicycles, scooters, motorcycles, and current ATV and UTV models. The hubless design that covers all these models is a very sleek and elegant design. Furthermore, the advantage of utilizing the difference in moment of inertia is a significant advantage.

CONFLICT OF INTEREST

The authors have no known conflict of interest or any shared interests with any institution, organization, or individual.

AUTHOR CONTRIBUTIONS

Veysel Türkel contributed to the identification and management of conceptual and design processes, while Said Bera Çivi played an active role in data collection, analysis, and interpretation.

REFERENCES

[1] Mopare, S., Patel, M., Bhosale, A., Detke, R., Bindu, R. (2018) Design and development of an innovative hubless wheel, IOSR Journal of Mechanical and Civil Engineering, 15(3), 01-14.
[2] http://sbarro.phcalvet.fr/, Erişim Tarihi: Ocak 2018, Konu: Franco Sbarro, Another Vision of Car 2000.
[3] RMK's hubless rear Wheel drive under contruction | Electric Vehicle Sbarro Orbital Wheel, 1929-Franco Sbarro
[4] Karayolunda Seyreden Araçlara Etkiyen Dirençler | Bölüm 4 (2009) Akdeniz Üniversitesi-Karayolları Müh.
[5] Mopare, S., Patel, M., Bhosale, A., Detke, R., Bindu, R. (2018) Design and development of an innovative hubless wheel, IOSR Journal of Mechanical and Civil Engineering, 15(3), 01-14.
[6] Bozacı, A., Koçaş, İ. ve Çolak, Ö. Ü. (1989) Makina Elemanlarının Projelendirilmesi. Seç Yayın Dağıtım, İstanbul.
[7] Trivini, R. (2010) Hubless castor wheel construction, particularly for furniture articles, U.S. Patent No. 7,657,969. Washington, DC: U.S. Patent and Trademark Office.
[8] Wang, X.P. ve Feng, L. inventors; Shanghai Magic Wheels Sporting Goods Co Ltd, assignee. Hubless wheel. United States patent US 9,573,417. 2017 Feb 21.